

University of Groningen

## A one-dimensional instationary heterogeneous mass transfer model for gas absorption in multiphase systems

Brilman, D.W.F.; Swaaij, W.P.M. van; Versteeg, G.F.

*Published in:*  
Chemical Engineering and Processing: Process Intensification

*DOI:*  
[10.1016/S0255-2701\(98\)00055-5](https://doi.org/10.1016/S0255-2701(98)00055-5)

**IMPORTANT NOTE:** You are advised to consult the publisher's version (publisher's PDF) if you wish to cite from it. Please check the document version below.

*Document Version*  
Publisher's PDF, also known as Version of record

*Publication date:*  
1998

[Link to publication in University of Groningen/UMCG research database](#)

### *Citation for published version (APA):*

Brilman, D. W. F., Swaaij, W. P. M. V., & Versteeg, G. F. (1998). A one-dimensional instationary heterogeneous mass transfer model for gas absorption in multiphase systems. *Chemical Engineering and Processing: Process Intensification*, 37(6), 471-488. [https://doi.org/10.1016/S0255-2701\(98\)00055-5](https://doi.org/10.1016/S0255-2701(98)00055-5)

### **Copyright**

Other than for strictly personal use, it is not permitted to download or to forward/distribute the text or part of it without the consent of the author(s) and/or copyright holder(s), unless the work is under an open content license (like Creative Commons).

The publication may also be distributed here under the terms of Article 25fa of the Dutch Copyright Act, indicated by the "Taverne" license. More information can be found on the University of Groningen website: <https://www.rug.nl/library/open-access/self-archiving-pure/taverne-amendment>.

### **Take-down policy**

If you believe that this document breaches copyright please contact us providing details, and we will remove access to the work immediately and investigate your claim.

Downloaded from the University of Groningen/UMCG research database (Pure): <http://www.rug.nl/research/portal>. For technical reasons the number of authors shown on this cover page is limited to 10 maximum.

# A one-dimensional instationary heterogeneous mass transfer model for gas absorption in multiphase systems<sup>1</sup>

D.W.F. Brilman \*, W.P.M. van Swaaij, G.F. Versteeg

*Department of Chemical Engineering, Twente University of Technology, P.O. Box 217, 7500 Enschede, The Netherlands*

Received 2 February 1998; accepted 2 May 1998

## Abstract

For a physically correct analysis (and prediction) of the effect of fine, dispersed phase drops or particles on the mass transfer rate in multiphase systems, it was demonstrated that only 3-D instationary, heterogeneous mass transfer models should be used. Existing models are either homogeneous, stationary or single particle models. As a first step, a 1-D, instationary, heterogeneous multi-particle mass transfer model was developed. With this model the influence of several system parameters was studied and problems and pitfalls in the translation of modeling results for heterogeneous models into a prediction of absorption fluxes are discussed. It was found that only those particles located closely to the gas–liquid interface determine mass transfer. For these particles the distance of the first particle to the gas–liquid interface and the particle capacity turned out to be the most important parameters. Comparisons with a homogeneous model and experimental results are presented. Typical differences in results comparing a homogeneous model with the 1-D heterogeneous model developed in this work could be attributed to a change in the near interface geometry. Future work in this field should therefore be directed towards near interface phenomena. Three dimensional mass transfer models, of which a preliminary result is presented, are indispensable for this. © 1998 Elsevier Science S.A. All rights reserved.

**Keywords:** Mass transfer enhancement; Heterogeneous model; Multiphase systems

## 1. Introduction

Three phase reactors, especially slurry reactors, are widely used in the chemical industries for a variety of processes. Frequently the absorption rate of a (sparingly) soluble gas phase reactant to the reaction phase is rate determining [1]. Experiments have shown that the gas–liquid mass transfer rate may be significantly enhanced by the presence of a third, dispersed, phase. This phenomenon can be attributed to the diffusing reactant which either absorbs preferentially or is consumed by a chemical reaction [2,3]. The dispersed phase can be solid (adsorbing or catalyst) particles or liquid droplets.

Among others Kars et al. [2] and Alper and Deckwer [4] have shown experimentally that the addition of fine

particles to a gas–liquid system caused an enhancement of the specific gas absorption rate (per unit of driving force and interfacial area), whereas larger particles showed almost no effect. Owing to a particle size distribution also in applications where the mean particle diameter is relatively large, a significant enhancement of the gas absorption rate may be observed. This was confirmed experimentally by Tinge and Drinkenburg [5], who added very fine particles to a slurry consisting already of larger ones and found that the enhancement of gas absorption to be similar to the enhancement of the gas absorption rate due to the addition of only the same amount of fine particles to a clear liquid.

Such size distributions will certainly occur in case of gas absorption (or solids dissolution) in a liquid–liquid dispersion. Nishikawa et al. [6] have shown for liquid–liquid systems that the effect of aeration is a broadening of the droplet size distribution, i.e. more fine droplets. This implies that especially for gas–liquid–

\* Corresponding author. Tel.: +31 53 4894479; fax: +31 53 4894774.

<sup>1</sup> This contribution is dedicated to the remembrance of Professor Jacques Villermanx.

liquid systems, enhancement of gas absorption can be expected when, of course, the solubility of the diffusing component in the dispersed liquid phase exceeds the solubility in the continuous liquid phase.

The presence of these small particles does not only lead to significantly higher absorption rates (up to a factor 10), enabling smaller process equipment, but also selectivity in multistep reaction systems may be affected. In some applications a dispersed phase is added on purpose to a two phase system in order to reduce mass transfer limitations [7,8].

Since the effect of the presence of a dispersed phase on mass transfer can be significant, knowledge on the mass transfer mechanism and a model to predict this enhancement effect is desirable.

The increase of the specific gas absorption rate, at unit driving force and unit interfacial area, due to the presence of the dispersed phase can be characterized by an enhancement factor,  $E$ . This enhancement factor is defined as the ratio of the absorption flux in the presence of the particles to the absorption flux at the same hydrodynamic conditions and driving force for mass transfer without such particles, respectively.

Using the definition above, possible effects of the presence of particles on the gas–liquid interfacial area and on local hydrodynamics are taken into account. For a complete and more detailed review the reader is referred to Beenackers and van Swaaij [1].

The enhancement of the specific absorption flux due to the presence of fine particles has been explained by the so-called ‘grazing-’ or ‘shuttle-’ mechanism [2,9]. According to this shuttle-mechanism, particles pendle frequently between the stagnant mass transfer zone at the gas–liquid interface and the liquid bulk. Due to preferential adsorption of the diffusing gas phase component in the dispersed phase particles, the concentration of this gas phase reactant in the liquid phase near the interface will be reduced, leading to an increased absorption rate. After a certain contact time, the particle will return to the liquid bulk where the gas phase component is desorbed and the particles regenerated. This shuttle mechanism requires that the dispersed phase particles are smaller than the stagnant mass transfer film thickness,  $\delta_F$  according to the film theory. For gas absorption in aqueous media in an intensely agitated contactor a typical value for  $\delta_F$  is  $\approx 10$ – $20$   $\mu\text{m}$ , whereas for a stirred cell apparatus this value is typically about a few hundred micron.

In the present study, multiphase systems with a finely dispersed phase will be considered, so that one or more dispersed phase ‘particles’ (which can either be liquid drops or solid particles) may be present within the stagnant film thickness at the gas–liquid interface. This is represented in Fig. 1.

A diffusing solute now may or may not encounter one or more droplets when diffusing into the composite

medium. From the pioneering modeling work by Holstvoogd et al. [10], who studied stationary diffusion into a series of liquid cells, each containing one catalyst particle, it became clear that especially those particles which are located most closely to the gas–liquid interface affect mass transfer. This implies that local geometry effects at the gas–liquid interface as for example the position of the particles with respect to the interface and with respect to each other (‘particle–particle interaction’) will influence the observed mass transfer enhancement.

The effect of the solubility (or equivalently, the adsorption capacity) of the dispersed phase for the diffusing solute was investigated by Holstvoogd and van Swaaij [11] and Mehra [12], both using an instationary, penetration theory based, homogeneous model for gas-absorption. It was found that particles with a low capacity (i.e. a low relative volumetric solubility  $m_R$  or adsorption capacity) easily get saturated and do not contribute any longer to the enhancement of gas–liquid mass transfer. For this reason, stationary models, like the film model, which neglect the accumulation are inappropriate.

Models reported so far in literature are either homogeneous models (neglecting geometry effects and mass transfer inside the dispersed phase), heterogeneous stationary models (only applicable for very high capacity particles located very close to the gas–liquid interface) or 1-D, one particle models. These models will be discussed briefly in Section 2.

However, to describe the effect of dispersed phase particles on gas absorption accompanied by chemical reaction it seems more realistically to develop instationary, 3-D, heterogeneous, multi-particle, mass transfer models.

As a first step in this, an instationary heterogeneous, 1-D, multi-particle model will be developed, which is the aim of the present contribution. With the present model, first the influence of a single particle to the gas absorption enhancement will be studied. The particle-to-interface distance, particle capacity, diffusion coefficient ratio and chemical reactions are varied. Further, multiparticle simulations will be presented. The cou-

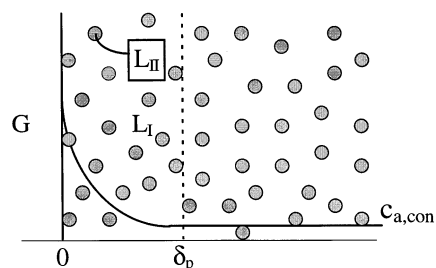


Fig. 1. Fine dispersed phase droplets located within the penetration depth  $G$ , gas phase;  $L_I$ , continuous phase;  $L_{II}$ , dispersed phase.

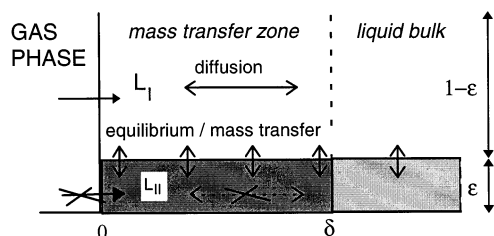


Fig. 2. Typical representation of a homogeneous model.

pling of modeling results with absorption rate or flux predictions will be discussed and a comparison with experimental data from literature and with homogeneous models already available in literature will be presented.

## 2. Previous work

For describing the phenomenon of gas absorption in the presence of dispersed phase particles in the mass transfer zone, several approximation models have been developed in the past. The first models developed were the homogeneous models, see e.g. the work of Bruining et al. [13], Mehra [14], Littel et al. [15] using the penetration theory or Nagy and Moser [16] who used the film-penetration theory. Homogeneous models represent the situation of Fig. 1 by taking a constant fraction ( $\varepsilon$ ) of the film to be occupied by the dispersed phase. A typical representation of a homogeneous model is given in Fig. 2.

Bruining et al. [13] and Kars et al. [2] neglected any mass transfer resistance in or around the dispersed phase droplets and estimated the mass transfer enhancement factor  $E$  just by accounting for the increased solubility (capacity) of an effective homogeneous liquid through Eq. (1a), in which  $m_R$  is the volume based solubility ratio of the solute over the dispersed phase and the continuous phase.

$$E = \sqrt{1 + \varepsilon(m_R - 1)} \quad (1a)$$

The estimation of 'a maximum attainable enhancement factor' for absorption in emulsions, based on the penetration theory, was proposed by van Ede et al. [17], see Eq. (1b). In this equation,  $D_R$  is the ratio of the diffusion coefficients and represents the effect of complete parallel diffusional transport through the dispersed phase.

$$E = 1 + \varepsilon(m_R \sqrt{D_R} - 1) \quad (1b)$$

The latter equation, however, is only valid for liquid–liquid dispersions.

In Fig. 2, the dispersed phase is depicted as a separate homogeneous phase, which may offer a parallel transport route to the diffusing solute. The variations

between different homogeneous models presented in literature are due to the description of mass transfer towards and inside this dispersed phase. Nagy and Moser [16] among others accounted for the mass transfer resistance within the dispersed phase, which is neglected in most other models [14]. Littel et al. [15] accounted for diffusion through the dispersed phase droplets by introducing an effective diffusion coefficient for the composite medium into the homogeneous model.

Since spherical droplets or particles can for the asymptotic situation only 'touch' the gas–liquid interface, the dispersed phase hold-up in this region will vary with the position in the mass transfer zone. Assuming the dispersed phase fraction at the interface to be at overall bulk liquid phase, conditions may in this case lead to an overestimation of the enhancement factor by the homogeneous models. This effect was recognized by van Ede et al. [17], who tried to account for this local geometry effect in this region by varying the dispersed phase hold-up from zero hold-up at the gas–liquid interface to the average bulk liquid phase hold-up at a distance  $x \geq d_p$  from the gas–liquid interface. To arrive at a good agreement with the experimental data parallel diffusion through the dispersed phase was introduced in their modified film model.

Due to their 1-D character, all homogeneous models only consider diffusion perpendicular to the gas–liquid interface. However, particles close to the interface diffusion in other directions than perpendicular to the gas–liquid interface, may also be very important. In this case the effect on mass transfer is probably underestimated by the homogeneous models. A homogeneous description of the dispersion is clearly physically not very realistic and may therefore lead to erroneous results for more complex situations.

Pioneering work in developing heterogeneous 3-D, one particle, models was done by Holstvoogd et al. [10] and Karve and Juvekar [18]. Both developed stationary heterogeneous models for the description of gas absorption in slurry systems with an (infinitely) fast, irreversible chemical reaction at the solid surface. From their results it became clear that the distance of the particles to the gas–liquid interface was a major parameter determining the effect on the mass transfer rate. These models are, however, not very suitable for absorption in liquid–liquid dispersions because they do not allow for diffusion through the dispersed phase. Furthermore, the model of Karve and Juvekar [18] assumes an infinite capacity of the particles, thus neglecting the effect of saturation, and the particle position was fixed at the center of the unit cell. Additionally, their model overestimates the effect of neighboring particles, due to the cylindrical geometry of the unit cell applied with a symmetry boundary condition. In the model of Holstvoogd et al. [10] the particle

position was also chosen rather arbitrarily at the center of the unit cell.

Instationary, 1-D, heterogeneous one particle models were proposed by Junker et al. [7,8] and Nagy [19]. In the model by Junker et al. [7,8], based on the penetration theory, a droplet can only partially fit within penetration depth for mass transfer, reflecting the rather large droplet sizes  $d_p$  in their experimental system with respect to the calculated penetration depth  $\delta_p$  ( $d_p > \delta_p$ ). In the model by Junker et al. [7,8], the droplets are considered to be cubic, in order to maintain the 1-D character, having an equal volume to the spherical droplets ( $d = d_p \cdot (\pi/6)^{1/3}$ ) (Fig. 3). In their model each dispersed phase drop in the model (with diameter  $d$ ) is considered to have a 'sphere' of continuous phase surrounding it (total diameter  $d + R_D$ ). Using the volume fraction  $\epsilon_{dis}$ , the thickness of the continuous phase shell can easily be calculated via Eq. (2a).

The gas phase reactant may or may not encounter such a dispersed phase droplet when diffusing into the liquid dispersion. Both pathways,  $J_1$  and  $J_2$ , are indicated in Fig. 3. Clearly, the contribution of both pathways,  $J_1$  and  $J_2$ , should depend on the drop size and dispersed phase hold-up. According to Junker et al. [7,8] the fractional contribution of  $J_2$  to the total absorption flux can be estimated by  $d^2/(R_D + d)^2$ , based on the projected frontal area. The distance of the dispersed phase to the gas–liquid interface was chosen arbitrarily to be equal to  $R_D$  (though  $R_D/2$  probably would have been more consistent).

The specific absorption flux when the diffusing solute encounters a droplet,  $J_2$ , is calculated by an analytical expression for instationary diffusion through a 'plate' of the continuous phase followed by an semi-infinite medium of the dispersed phase [20], restricting the application of the model to physical mass transfer and zero and first order chemical reactions.

$$R_D = d \cdot (\epsilon^{-1/3} - 1) \quad (2a)$$

$$J_{total} = J_1 \cdot \left( \frac{d^2}{(d + R_D)^2} \right) + J_2 \cdot \left( 1 - \frac{d^2}{(d + R_D)^2} \right) \quad (2b)$$

The approach of Nagy [19] is in many aspects similar to the one of Junker. However, Nagy used the film-penetration model to derive analytical solutions for the

situation described in the model of Junker et al. [7,8] and for the cases in which the single particle is entirely located within the mass transfer zone. The spacing between drops is the same in each spatial variable and calculated by Eq. (2a).

Since the particle may fit entirely within the mass transfer film two liquid–liquid phase boundaries may be encountered by the diffusing solute. The analytic solutions derived by Nagy for the different cases are therefore significantly more complex, when compared to the model by Junker. For particles which are located completely within the penetration film thickness  $\delta_p$ , an averaging technique is required to account for the statistical probability of finding the particle at a certain position. Nagy [19] assumed equal probability of finding the particle in the range 0 to  $(\delta_p - d_p)$ , see Eq. (3b). For the total absorption flux Eqs. (3a) and (3b) are used:

$$J_{het} = j^{av} \epsilon^{2/3} + J_1 (1 - \epsilon^{2/3}) \quad (3a)$$

and

$$j^{av} = \frac{1}{\delta - d_p} \int_0^{\delta - d_p} J_2 dL \quad (3b)$$

with  $L$  the distance to the gas–liquid interface.

### 3. Development of a heterogeneous 1-D, instationary, multiparticle model

#### 3.1. Model assumptions

For the modeling of a gas–liquid absorption process, a basic physical mass transfer model must be chosen to describe the absorption process. Well known one parameter models include the film model, the penetration models of Higbie and the Danckwerts surface renewal model [21]. Two parameter models as the film-penetration model may also be used. As mentioned before, due to the finite capacity of the dispersed phase droplets a stationary model, like the film model, is not appropriate. For the homogeneous models Mehra [14] compared the Higbie penetration model and the Danckwerts surface renewal model and found comparable results. In the present work the Higbie penetration model was used, though the surface renewal model can also be implemented.

In the present study it is assumed that the characteristic contact time at the gas–liquid interface for liquid packages also applies for the dispersed phase particles, i.e. emulsion packages at the gas–liquid interface are replaced completely by new emulsion packages from the liquid bulk after a certain contact time  $\tau$ .

For comparison of heterogeneous simulation results with experimentally determined absorption rates, a proper implementation of the experimental conditions

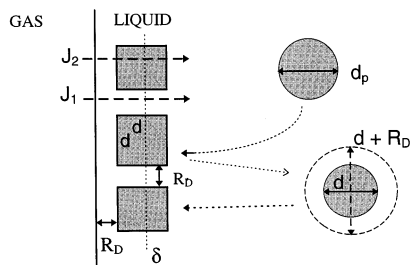


Fig. 3. Heterogeneous model by Junker et al. [7,8].

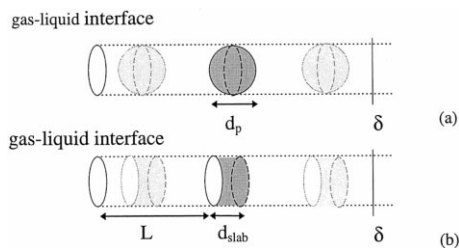


Fig. 4. From spherical particles within the penetration depth to a 1-D model representation.

into the model is required. Especially the representation of the dispersed phase hold-up  $\varepsilon$ , the particle size (distribution)  $d_p$  and the choice of a statistical function for the particle position is thereby important. In the present study the following procedure is proposed for this model representation.

Consider a 'cylinder' of the dispersion, perpendicular to the gas-liquid interface, with a diameter equal to the diameter of the spherical particle (Fig. 4(a)). For a correct representation of the volume fraction dispersed phase it can be derived that the number of particles within the mass transfer penetration depth should be equal to  $3/2 \cdot \varepsilon \cdot \delta_p / d_p$ . Fig. 4(a) is, however, still not a 1-D model since the diffusion path through the dispersed phase particle varies with the radial position. In order to arrive at a 1-D representation the spherical particles are replaced by a slab of equal volume (and thus equal absorption capacity). This leads to  $d_{slab} = 2/3 \cdot d_p$ , which is represented in Fig. 4(b). With this, the number of slabs (particles) in the unit cell is thus equal to  $N = \varepsilon \cdot \delta_p / d_p$ . The situation  $N < 1$  may be accounted for by taking the average of the results with cells with no particles and with one particle. For the positions of the particles it is assumed that the probability of finding a particle at a certain position from the interface is equal for every position.

One might have some objections with this representation of the absorption process in the dispersion, since the diffusing solute cannot bypass the dispersed phase particles. It should, however, be realized that due to the instationary character of the process and the statistical distribution of the particles over the penetration depth, still considerable absorption will take place, even in the case of impermeable solids. This particular situation will be investigated further on.

### 3.2. Model equations

In Fig. 5(a), a graphical representation of the 1-D model is given. In Fig. 5(a), the gas phase is located on the left hand side,  $L_I$  represents the continuous liquid phase and  $L_{II}$  the dispersed liquid phase

droplets. The parameter  $\delta_p$  is the penetration depth for mass transfer, as estimated by Higbie's penetration theory for physical absorption in the continuous phase ( $\delta_p = 2\sqrt{\pi D_c \tau}$ ). The actual penetration depth in the simulation of absorption in a dispersion package will, in general, differ from  $\delta_p$  due to a different volumetric absorption capacity of the dispersed phase droplets and the usually different diffusion coefficient within the dispersed phase particles. The model equations, initial conditions (IC) and boundary conditions (BC) for diffusion (with or without chemical reaction in one of the phases) are listed below for the diffusing solute 'a':

in the continuous phase:

$$\frac{\partial c_{a,c}(x,t)}{\partial t} = D_{a,c} \left( \frac{\partial^2 c_{a,c}(x,t)}{\partial x^2} \right) + R_{a,c} \quad (4a)$$

in the dispersed phase:

$$\frac{\partial c_{a,d}(x,t)}{\partial t} = D_{a,d} \left( \frac{\partial^2 c_{a,d}(x,t)}{\partial x^2} \right) + R_{a,d} \quad (4b)$$

$$\text{IC: } t = 0 \quad x \geq 0 \quad c_{a,c} = c_{a,d} = 0$$

$$(\text{or } c_{a,c} = c_{a,c,\text{bulk}} \text{ and } c_{a,d} = c_{a,d,\text{bulk}}) \quad (5)$$

$$\text{BC: } t > 0 \quad x = 0 \quad c_{a,c} = c_{a,c}^* \quad (\text{or } c_{a,d} = c_{a,d}^*) \\ x = 2 \cdot \delta_p \quad c_{a,c} = 0 \quad (\text{or } c_a = c_{a,c,\text{bulk}}).$$

At the continuous phase-dispersed phase interfaces:

$$D_{a,c} \frac{dc_{a,c}}{dx} = D_{a,d} \frac{dc_{a,d}}{dx} \quad (6a)$$

$$c_{a,d} = m_{R,c} c_{a,c} \quad (6b)$$

At phase boundaries the continuity of mass flux and the distribution of the solute between the phases is accounted for through Eqs. (6a) and (6b). This is indicated in Fig. 5(b), where the computational grid around one of the dispersed phase particles is shown.

The terms,  $R_{a,c}$  and  $R_{a,d}$ , which account for possible occurring reactions can be any arbitrary kinetic expression. In case liquid phase reactants are also involved, similar diffusion/reaction equations have to be added and solved simultaneously. The initial and boundary conditions for non-volatile liquid phase reactants (here: component 'b') are then given by Eq. (7).

$$\text{IC: } t = 0 \quad x \geq 0 \quad c_{b,c} = c_{b,c,\text{bulk}},$$

$$c_{b,d} = c_{b,d,\text{bulk}} = m_{R,b} \cdot c_{b,c,\text{bulk}} \quad (7)$$

$$\text{BC: } t > 0 \quad x = 0 \quad D_{b,c} \frac{\partial c_{b,c}}{\partial x} = 0, \quad D_{b,d} \frac{\partial c_{b,d}}{\partial x} = 0$$

$$x = 2 \cdot \delta_p \quad c_{b,c} = c_{b,c,\text{bulk}}, \quad c_{b,d} = c_{b,d,\text{bulk}} = m_{R,b} \cdot c_{b,c,\text{bulk}}$$

The above presented model, which was solved numerically using an Euler explicit finite difference method, can be used to explore mass transfer enhancement effects in multiple phase systems. The number of particles as well as their sizes and their positions can

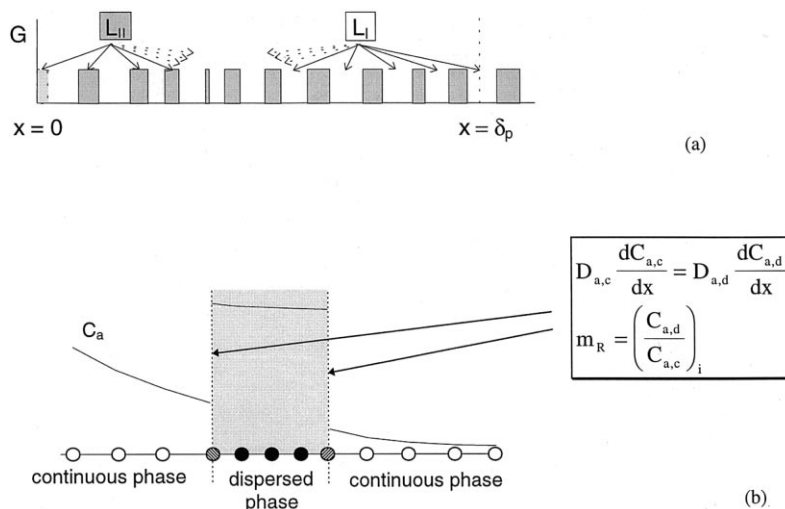


Fig. 5. The 1-D, instationary, multi-particle model. (a) Graphical representation of a multiparticle cell. (b) Computational grid around one droplet.

be varied arbitrarily. Direct gas-dispersed phase contact can be implemented by placing a particle at the gas–liquid interface; i.e. the distance between the interface and the first dispersed phase particle is equal to zero.

From the model the specific rate of absorption, which is time dependent,  $J(t)$  in (mol m<sup>-2</sup> per s), and the average specific rate of absorption over the gas–liquid contact time,  $J_{av}(\tau)$  in (mol m<sup>-2</sup> per s), are obtained. The enhancement factor is defined by the ratio of these fluxes to their equivalent for gas absorption under identical conditions without the presence of a dispersed phase, see Eq. (8a,b).

$$E(t) = \frac{J(t)}{\sqrt{\frac{D_c}{\pi t}}}, \quad E_{av}(\tau) = \frac{J_{av}(\tau)}{2\sqrt{\frac{D_c}{\pi \tau}}} \quad (8a,b)$$

The enhancement factors  $E$  mentioned refer always to the contact time averaged enhancement factor  $E_{av}(\tau)$ , unless mentioned otherwise. The model was validated against analytical solutions for physical absorption and for absorption accompanied by homogeneous chemical reaction in the continuous phase for situations without particles. After adapting the model to the geometry described by Junker et al. [7,8] the results were also validated with the analytical solutions for  $J_2$  in their model.

## 4. Simulation results

### 4.1. Single particle simulations

Simulations are carried out in which the beforehand, identified as most relevant model parameters, were varied for the case of only one particle present within the mass transfer penetration depth. The main goal is to investi-

gate the sensitivity of the model calculations for the parameter variations.

The influence of the following parameters were studied:

- particle position.
- ‘particle capacity factors’, including the relative solubility  $m_R$  and relative diffusivity  $D_R$ .
- first order irreversible reactions in the continuous phase and in the dispersed phase.

Bimolecular reactions and special reactions as parallel, consecutive and autocatalytic reactions can easily be implemented in the model, but these situations are not included in the present study. Results from this 1-D heterogeneous model with one particle may be useful for translating simulation results into absorption flux predictions. Therefore, in these simulations the default values for the model parameters involved refer to the conditions taken from the experiments by Littel et al. [15] and, additionally, in all simulations an unloaded liquid bulk solution was considered. In next sections the parameter  $\delta_p$  is sometimes used as a scaling factor. This parameter  $\delta_p$  refers to the penetration depth at identical conditions for the absorption, but in absence of the particle(s).

#### 4.1.1. Particle position

In the work of Holstvoogd et al. [10] it was clearly demonstrated that the particle position is one of the major parameters. With the present model, a few simulations were performed in which the particle size was varied. If the particles were located at the same distance from the gas–liquid interface, the absorption rates calculated were almost identical, but if the position of the centers of the particles was kept constant, the larger particles, being more close to the interface, showed a much higher enhancement factor. It was concluded that especially the distance of the particle to the interface,  $L$ ,

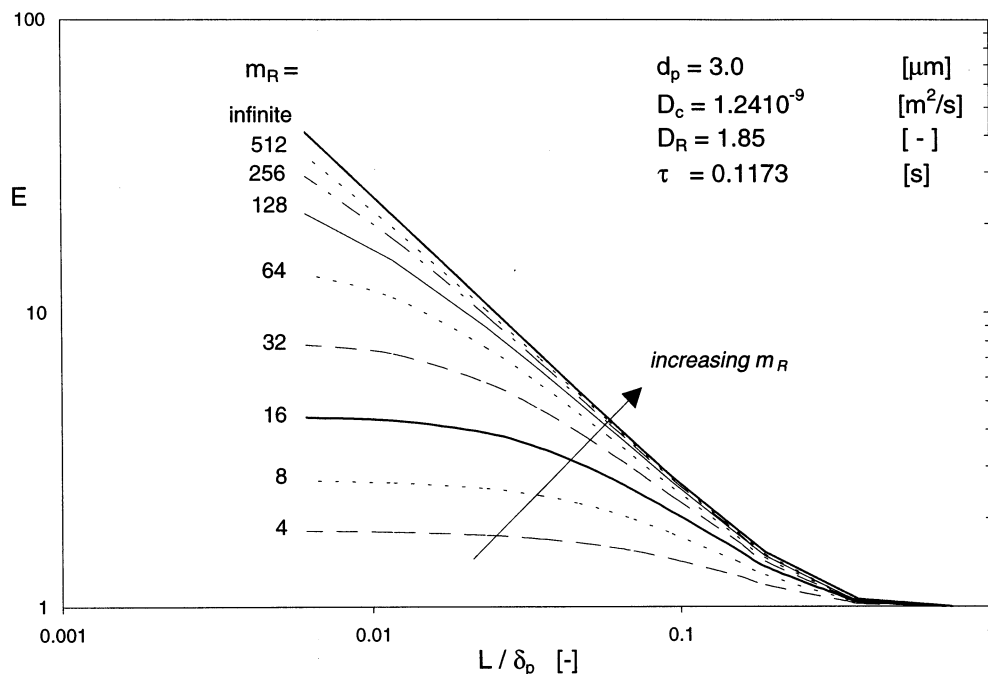


Fig. 6. Single particle calculations: Variation of position and relative solubility.

is important in determining the effect on the absorption rate.

Since the relative solubility of the diffusing solute in the particle is also very important, Eq. (1a), and saturation effects may be important the influence of the distance of the particle to the gas–liquid interface is studied for finite and infinite capacity particles. For finite capacity particles the enhancement factors as functions of  $L$  for different values of the relative solubility parameter  $m_R$  are shown in Fig. 6. In this plot the  $L$  value was scaled with respect to  $\delta_p$ , since it was found that by changing  $D_c$ ,  $d_p$  and  $t$ , identical results were found if  $L/\delta_p$  and  $d_p/\delta_p$  were kept constant. From these results it is clear that the enhancement factor is quite sensitive to the parameter  $(L/\delta_p)$ . Above values for  $(L/\delta_p)$  of 0.3 almost no enhancement is calculated.

In case of a high relative volumetric solubility  $m_R$  or an instantaneously fast, irreversible  $n$ th-order reaction for the diffusing solute (no other components involved) in the dispersed phase droplet or at the surface of a solid catalyst particle, the particle capacity may be considered infinite. In these cases the following simple correlation was found to describe the enhancement factor with reasonable accuracy (average deviation  $\approx 1\%$  in the relevant range  $0-0.3 \cdot \delta_p$ , maximum deviation  $(\Delta E) \pm 0.1$  unit at  $L = 0.5 \cdot \delta_p$ ):

$$E^2 = \frac{15}{16} + \left( \frac{\delta}{4L} \right)^2 \quad (9)$$

For high capacity particles ( $m_R > 1000$ ) located sufficiently close to the gas liquid interface the enhancement factor can be estimated as function of the position  $L$  by

this equation. Deviations are less than 10% if the degree of saturation of the particles is less than 10%.

Note that Eq. (9) cannot be used for a situation in which there is direct gas-dispersed phase contact ( $L = 0$ ). In these cases mass transfer will be determined by transport within the dispersed phase and in the gas phase.

#### 4.1.2. Particle capacity

Next to the distance of the (first) particle to the interface, it is clear from Fig. 6 that the ‘capacity’ of the particle plays a significant role in the mass transfer enhancement. Particles having a low relative solubility factor ( $m_R$ ) will be faster ‘saturated’ during the gas–liquid contact time. These particles do not further enhance the mass transfer by acting as a sink for the gas phase component. This effect is demonstrated in Fig. 7, where the ‘momentary’ enhancement factor is plotted during the contact time. For ‘saturated’ particles the relative diffusion coefficient  $D_R$  of the gas phase component in the dispersed phase then determines whether gas–liquid mass transfer is enhanced or retarded, when compared to absorption into liquid phase in the absence of particles. Particle capacity will depend on the relative solubility  $m_R$  and the particle size  $d_p$ . For the degree of saturation which will be reached within the contact time also the position of the particle with respect to the interface is important.

For the particles affecting mass transfer, located close to the interface, it can be assumed that a linear concentration profile for diffusion to the first dispersed phase particle will be reached in short time. Neglecting



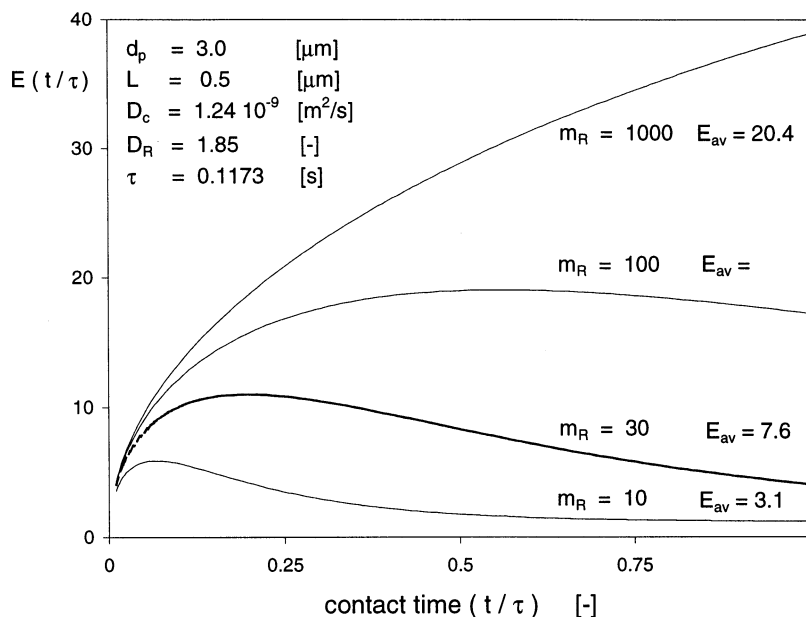


Fig. 7. Momentary enhancement factors during the gas–liquid contact time.

mass transfer resistances within the dispersed phase and mass transfer out of the dispersed phase ‘at the back of the particle’, the following expression for the degree of saturation, which will be reached within the characteristic contact time  $\tau$ , can be derived.

$$\left( \frac{C_d}{m_R C_c^{\text{ref}}} \right) = 1 - e^{-D_c \tau / m_R L d_p} = 1 - e^{-1/2 \pi m_R (L/\delta_p) (d_p/\delta)} \quad (10)$$

In this equation  $C_c^{\text{ref}}$  is the concentration at the same distance from the gas–liquid interface during (physical) absorption in the liquid phase without particles present at further identical conditions. The equation was found to describe this relative degree of saturation of the first particle within 5% deviation.

#### 4.1.3. Diffusion through the particles

In the situation shown in Fig. 5(a), diffusion occurs alternating in the continuous and dispersed phase (similar to resistances in series). The diffusion coefficient in the dispersed phase will therefore affect the mass transfer process. This effect will only be significant for low capacity particles, when transport through the first particle(s) becomes important. From Fig. 8 it can be concluded that for one single, small, particle this effect is limited in practical situations, where  $0.1 < D_R < 10$ . Here also, the influence of the particle decreases with increasing distance to the gas–liquid interface. In the legend the limiting value for  $E$  in case of impermeable solids is given for a few values of  $L$ , under the conditions mentioned.

#### 4.1.4. Effect of contact time $\tau$

The characteristic average contact time  $\tau$  was

varied over a broad range to investigate its effect on the mass transfer enhancement factor,  $E_{av}(\tau)$ , due to the presence of a single particle, located at different positions from the gas–liquid interface. This may represent e.g. the effect of an increasing stirring rate in agitated systems. Results are presented in Fig. 9. With this, the importance of the effect of the contact time on the enhancement factor is shown. Since the simulations are carried out for particles of given size  $d_p$  at fixed distances  $L$  from the gas–liquid interface the characteristic geometrical parameters  $d_p/\delta_p$  and  $L/\delta_p$  vary through  $\delta_p$ , which solely depends on  $\tau$  for a given set of physical properties ( $m_R$ ,  $D_R$  and  $D_c$ ). With this, the maximum in these curves can be understood. For a given particle position ( $L/\delta_p$ ) will decrease with increasing contact time, resulting in higher enhancement factors. For very low values of  $L/\delta_p$  the particle is saturated relatively fast and does not contribute any longer significantly to the mass transfer enhancement and  $E$  decreases again. These curves can further be used to evaluate average absorption fluxes using a surface renewal model. For a few particle positions these data were used to calculate the enhancement factor using the surface renewal model. Differences between the penetration model and surface renewal model results were found to be maximally 10%.

#### 4.1.5. First order, irreversible chemical reactions in the dispersed and continuous phase

The effect of a chemical reaction which shows first order reaction kinetics with respect to the gas phase component was investigated separately for the reac-

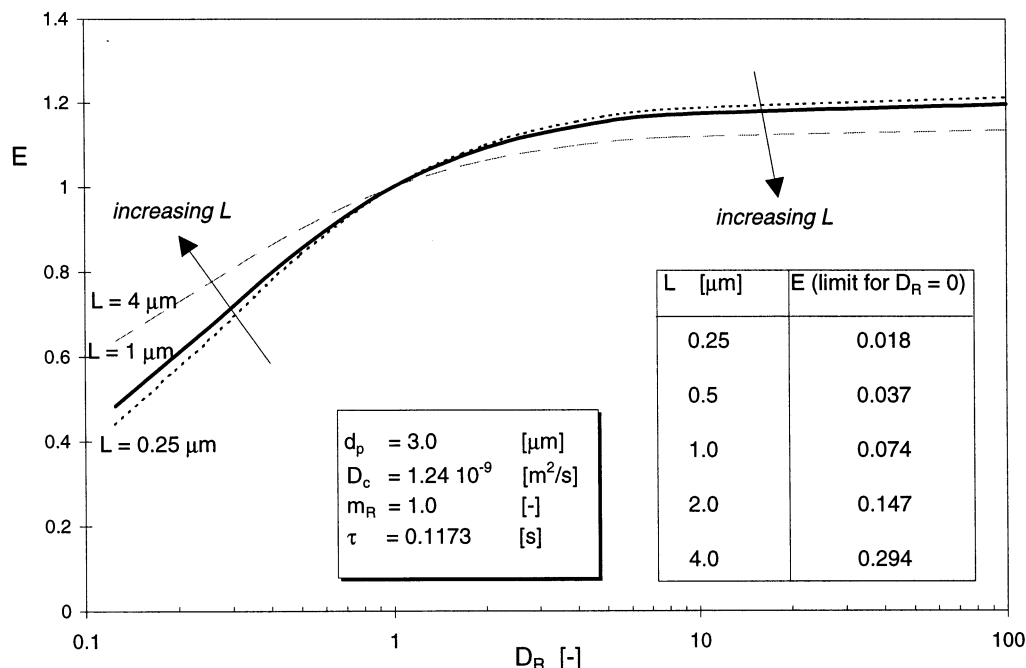


Fig. 8. Influence of the dispersed phase permeability on the enhancement factor  $E$  for a single particle.

tion occurring in the dispersed phase and in the continuous phase. Increasing the reaction rate constant for an irreversible first order reaction located in the dispersed phase should increase the absorption flux, until the 'infinite enhancement factor' due to the presence of the dispersed phase particle at a certain position is reached. In that case the capacity of the dispersed phase droplet can be considered infinite and the enhancement factor can be approximated by Eq. (9). The degree of saturation will be then be low. It was found that this is achieved for  $m_R \cdot (1 + k_{1,d}^{1/2})$  exceeding approximately the value 1000.

For a first order reaction in the continuous phase the penetration depth will decrease with increasing reaction rate constant ( $\delta' \approx \delta_p / E_{c,c}$ ), thereby reducing the probability to find particles within the mass transfer zone. Therefore, with increasing  $k_{1,c}$  value a diminishing effect of the overall mass transfer enhancement due to the presence of particles can be expected. The effect of  $k_{1,d}$  and  $k_{1,c}$  for a typical application is given in Fig. 10. Increasing  $k_{1,d}$  at a certain  $k_{1,c}$  value again increases the enhancement factor (at constant  $L/\delta'$  value) somewhat. The enhancement due to the presence of dispersed phase particles is a function of the ratio of the capacity of the particles to the capacity of the continuous liquid phase which is replaced by the particle

#### 4.2. Multiparticle calculations

For the conditions mentioned in Table 1, calculations were performed for a multi-particle situation. The position of the particles is shown in the concentration

versus  $x$ -position graph of Fig. 11(a), where the concentration within the dispersed phase is taken as the relative value with respect to its maximum solubility. From this figure it is clear that with increasing  $m_R$  the penetration depth decreases and fewer particles are located within the actual penetration depth. Thus only those particles located closely to the gas–liquid interface will cause the gas absorption enhancement. At high  $m_R$  values (and  $D_R = 1.85$ ) the concentration within the particles is almost uniform; the resistance for mass transfer is located almost exclusively in the continuous liquid phase. For  $m_R$  values  $< 1$ , the major resistance for mass transfer is located within the dispersed phase particles. To maintain a certain flux (see also Eqs. (6a) and (6b)), through the particles the concentration gradient within the particles will be much steeper in these cases. The calculated enhancement factors for the particle configuration shown in Fig. 11(a) are plotted versus the relative solubility of solute A in the dispersed phase in Fig. 11(b).

For the case of  $m_R = 1$ , also the value of  $D_R$  was varied between 0.1 and 100. At  $D_R = 0.1$  the 'enhancement' factor calculated was 0.81, whereas for  $D_R = 100$  the enhancement factor was only 1.04. The negligible enhancement effect can be understood using the results presented in Fig. 8, considering that in this case the dispersed phase fraction is only 0.10 and the value of  $L/\delta_p$  is relatively large ( $L/\delta_p = 0.13$ ).

The importance of the first few particles near the gas–liquid interface is further stressed by multiparticle calculations in which subsequently one particle was added, until a similar situation as in Fig. 11(a) was

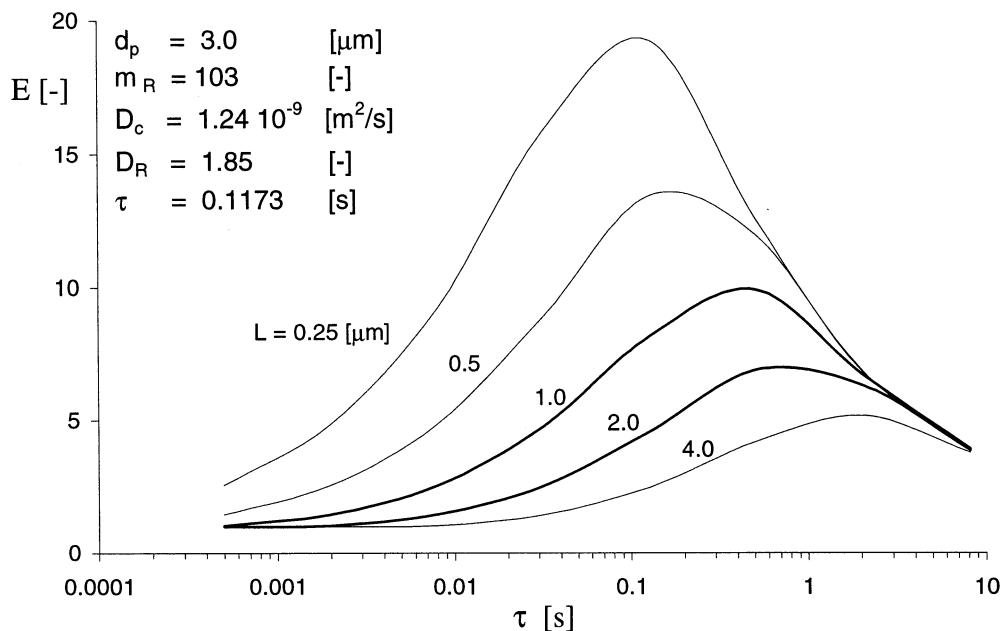


Fig. 9. Enhancement factors at varying contact times for different positions  $L$ .

obtained. The simulation data and obtained mass transfer enhancement factors for these cases are listed in Table 2. If the distance of the first particle to the interface is increased the additional enhancement due to the presence of a second particle (slightly) decreases (no data illustrating this are included).

### 5. Comparison with experimental results and with a homogeneous model

For a typical homogeneous model [13–15] the dispersed phase fraction, as well as the droplet size and relative solubility were varied. The results are presented in Fig. 12(a) and (b). From Fig. 12(b), e.g. the influence of the particle size on the calculated enhancement factor can be seen, being more important at high  $m_R$  values.

For the comparison of homogeneous and heterogeneous models both models, respectively were compared with experimental data for the mass transfer enhancement in liquid–liquid systems. In this work the data of Littel et al. [15] and of Mehra [14] were used. For the heterogeneous models it is required to average over all possible particle positions within the penetration depth. However, for the conditions used by Littel et al. [15] and Mehra [14], a multi-particle simulation showed that in good approximation only the first particle is really determining the gas absorption enhancement, which can also be deduced from the results of Table 2. This allows us to use single particle calculations.

Simulations were performed for one single particle present within the penetration depth  $\delta_p$  and using the

appropriate physico-chemical properties as given with the experimental data. The enhancement factors obtained for different positions of the particle,  $E(L)$ , were correlated. If  $N$  particles are present within the penetration depth, the distance of the first particle to the gas–liquid interface is likely to be within the range 0 to  $(\delta_p/N - d_p/2)$  ( $\mu\text{m}$ ). In estimating the experimental enhancement factor using the 1-D heterogeneous model, the single particle results were averaged over all possible positions within this section of the mass transfer zone:

$$\bar{E} = \frac{1}{\delta_p/N - d_p/2} \int_0^{\delta_p/N - d_p/2} E(L) dL \quad (11)$$

When more than one particle should be taken into account within the penetration depth (at high volume fractions of very small low capacity particles), the averaging procedure as proposed in Eq. (11) should be extended to all possible particle configurations. In good approximation, we believe this can be done in a sequential way. The first particle is most likely to be found at a distance 0 to  $(\delta_p/N - d_p/2)$  from the gas–liquid interface. Eq. (11) is now used to calculate the average enhancement due the first particle. The first particle is then fixed at a position for which the average enhancement factor is obtained. The next particle is most likely within the range  $(\delta_p/N - d_p/2)$  to  $2 \cdot \delta_p/N - d_p/2$  from the gas–liquid interface. Similar to Eq. (11), the average contribution of this second particle can be calculated. The second particle is then fixed at the position corresponding with that average contribution, and a third particle is considered, and so on. As may be clear

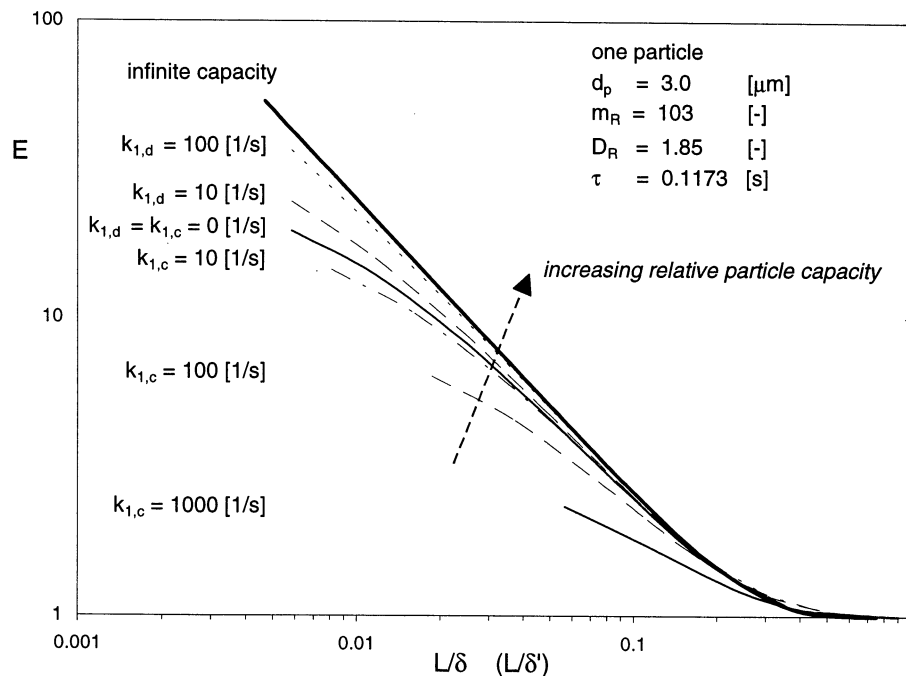


Fig. 10. Variation of the relative particle capacity through the first order reaction rate constant in the continuous phase and in the dispersed phase,  $k_{1,d}$ .

from Table 2(b) seldom more than four particles need to be taken into account.

With increasing the dispersed phase hold-up,  $\varepsilon$ , the number of particles within the penetration depth,  $N$ , increases and the first particle will, on the average, be located more closely to the interface. Consequently, the enhancement factor will increase. A comparison of some experimental results from literature with the calculated enhancement factors for the homogeneous and heterogeneous models are given in Table 3 and in Fig. 13.

Fig. 13 shows an almost linear increase of the enhancement factor with increasing hold-up for the heterogeneous model, whereas the homogeneous model shows a more 'logarithmic' dependency. For absorption in liquid–liquid emulsions this 'leveling off' of the enhancement factor with increasing dispersed phase hold-up can be recognized from the experimental data,

although the effect is less pronounced than predicted by the homogeneous models (see e.g. the work of van Ede et al. [17]). For solid catalyst particles (Pd on activated carbon) as dispersed phase, Wimmers and Fortuin [22] found the enhancement to increase linearly with the dispersed phase hold-up for experiments in a stirred tank reactor.

This difference in behaviour of the enhancement factor with increasing dispersed phase hold-up for the homogeneous model and the heterogeneous model can be explained via the position of the dispersed phase with respect to the gas–liquid interface. Varying the dispersed phase hold-up does not change the position of the dispersed phase in case of the homogeneous model (only increases the local fraction). For the heterogeneous model, however, the first particles will be located much closer to the gas–liquid interface with increasing hold-up. This effect causes the enhancement factor to increase almost linearly with the fractional hold-up of the dispersed phase. The importance of the position of the first particle is further illustrated by the data presented in Table 2(b). From this table it is clear that, when keeping the position of the first particle,  $L_0$ , fixed, the addition of more particles within the penetration depth does not contribute significantly to the absorption flux. When the influence of the addition of subsequent particles is simulated as increasing dispersed phase hold-up, the enhancement curves are leveling off (Fig. 14) which, however, is also found for the homogeneous models.

Table 1  
Conditions applied for the multiparticle calculations of Fig. 11

Particle diameter ( $d_p$ )	0.67 $\mu\text{m}$
Hold-up dispersed phase ( $\varepsilon$ )	0.10
Distance 1st particle to interface ( $L$ )	5.5 $\mu\text{m}$
Number of particles for $x = 0 \dots \delta_p$ ( $N$ )	6
Penetration depth without particles ( $\delta_p$ )	42.8 $\mu\text{m}$
Relative solubility ( $m_R$ )	103
Contact time ( $\tau$ )	0.1173 s
Diffusion coeff. Continuous phase ( $D_c$ )	$1.24 \cdot 10^{-9}$ $\text{m}^2$ per s
Diffusion coeff. Dispersed phase ( $D_d$ )	$2.30 \cdot 10^{-9}$ $\text{m}^2$ per s

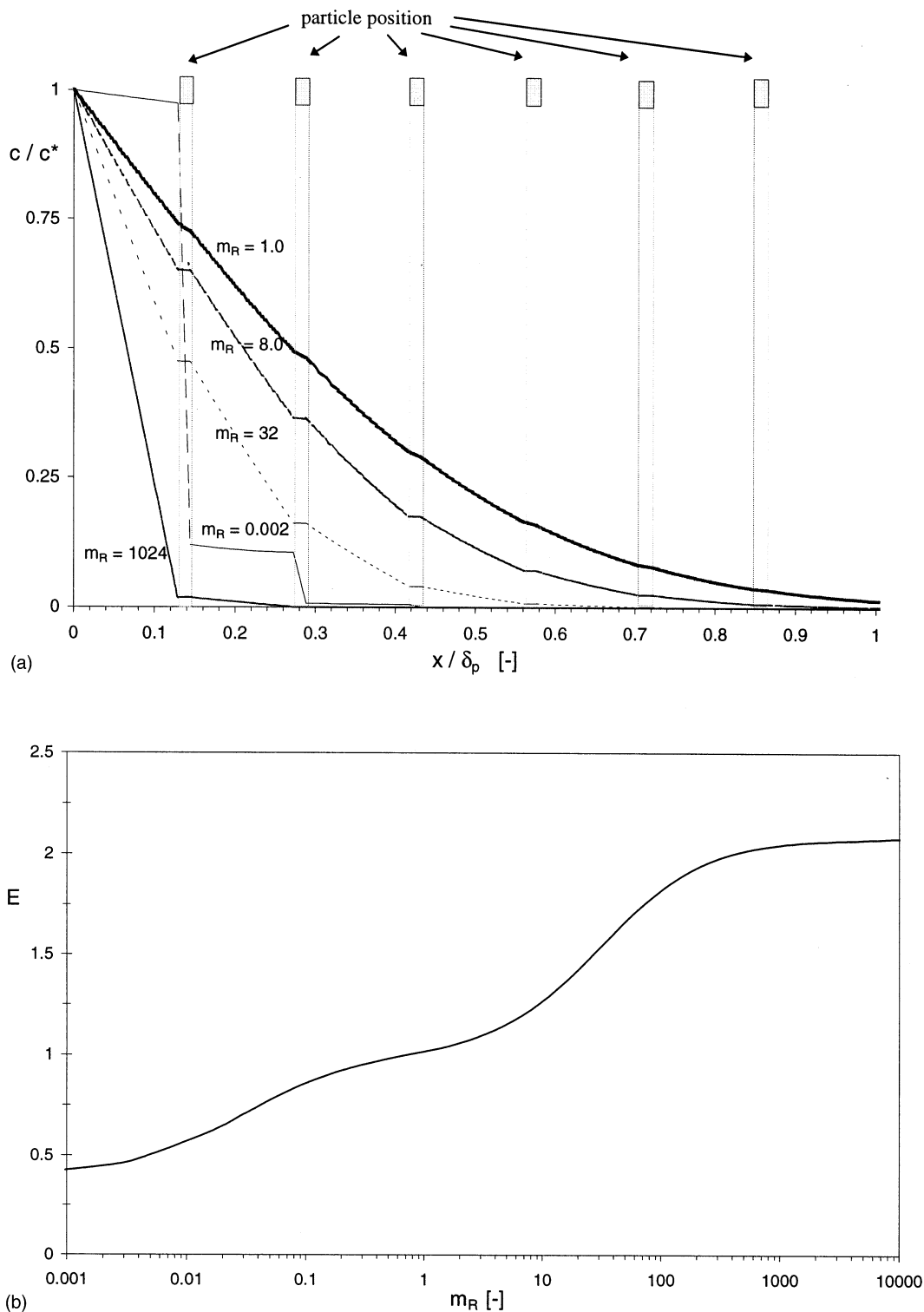


Fig. 11. (a) Concentration profiles within the penetration depth (for conditions see Table 1). (b) Enhancement factors vs. relative solubility (for conditions see Table 1).

The results of the simulations for the heterogeneous model are more sensitive to the particle size than the modeling results for the homogeneous model, which can be recognized from the Figs. 12 and 13. This is

again explained by the position of the first particle at the gas–liquid interface. At identical dispersed phase hold-up a decrease in particle size implies an increase in the number of particles and, with this, a decrease in the

Table 2

Effect of additional particles on the overall mass transfer enhancement

(a) Conditions applied						
Particle diameter ( $d_p$ )	2.0 $\mu\text{m}$					
Distance 1st particle to interface ( $L$ )	1.0 $\mu\text{m}$					
Penetration depth without particles ( $\delta_p$ )	42.8 $\mu\text{m}$					
Distribution coefficient ( $m_R$ )	4–100					
Contact time ( $\tau$ )	0.1173 s					
Diffusion coeff. (cont. phase) ( $D_{\text{con}}$ )	$1.24 \cdot 10^{-9}$ m <sup>2</sup> per s					
Diffusion coeff. (disp. phase) ( $D_{\text{dis}}$ )	$2.3 \cdot 10^{-9}$ m <sup>2</sup> per s					
Interparticle distance ( $L_{\text{pp}}$ )	2 $\mu\text{m}$					
(b) Simulation results						
No. particles	$m_R = 100$		$m_R = 10$		$m_R = 4$	
	$E$	$\Delta E/(E-1)$ (%)	$E$	$\Delta E/(E-1)$ (%)	$E$	$\Delta E/(E-1)$ (%)
0	1		1		1	
1	7.7072	(100)	2.2950	(100)	1.50492	(100)
2	7.8960	(2.7)	2.9893	(34.9)	1.85293	(40.8)
3	7.8977	(0.02)	3.1509	(7.5)	2.01666	(16.1)
4	7.8977	(0.02)	3.1725	(1.0)	2.06959	(4.9)
5			3.1744	(0.08)	2.08250	(1.2)
6			3.1745		2.08493	(0.2)
7			3.1745		2.08528	(0.03)

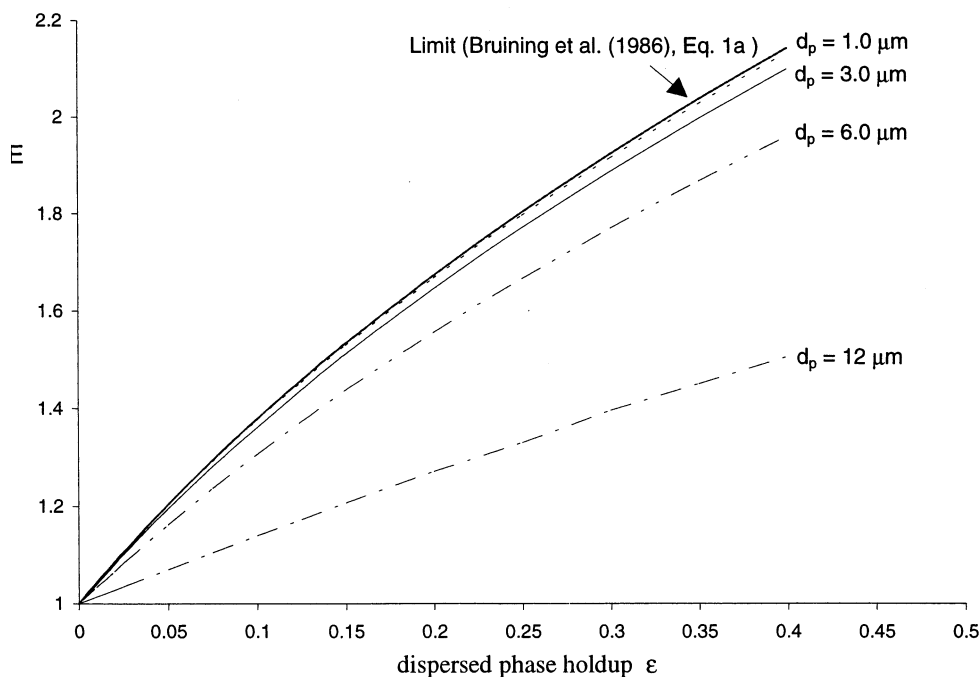
(averaged) distance of the first particle to the gas–liquid interface. For the same reason the average enhancement factor increases with a broadening of the particle size distribution at constant Sauter diameter. This may be essential in modeling the experiments by Mehra ([3]), who indicated ‘the droplet size lies in the range of 1 to 12  $\mu\text{m}$ , with a clustering around 3–4  $\mu\text{m}$ ’. The particle size distribution may very well be responsible for the deviations at high or low  $\varepsilon$ , due to the assumption of a mono-disperse particle size. Unfortunately, none of these experimental studies in literature presented more details on their specific dispersed phase particle size distribution.

Also in Table 3, a comparison between homogeneous and heterogeneous models is made for the situation of inert (impermeable and non-adsorbing) solid microparticles. This was studied experimentally by Geetha and Surender [23]. From their experimental results it is clear that, though undoubtedly significant differences were found for different types of solids, a considerable reduction of the mass transfer coefficient occurs at rather low volume fractions (at which viscosity effects due to the addition of the particles are negligible). From the modeling results it is clear that this effect is almost not identified in the simulations of the homogeneous models. The extent of this effect seems much better described by the heterogeneous model. It has to be mentioned that at larger volume fractions the mass transfer reduction tends to be overestimated by the heterogeneous model. This may be caused by neglecting lateral diffusion (bypassing of the particles). Simulations with 3-D heterogeneous models are necessary to support this explanation.

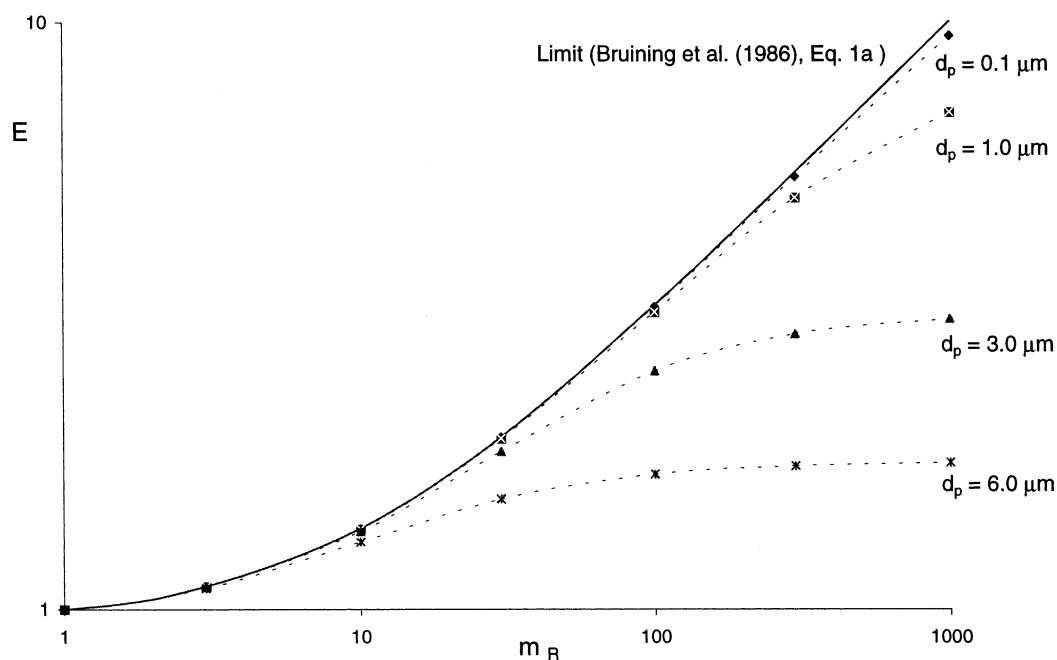
## 6. Discussion

From the comparison with experimental data it has become clear that a 1-D heterogeneous mass transfer model can reasonably predict absorption fluxes for situations in which the shuttle mechanism determines the mass transfer enhancement. Also the mass transfer retarding effect of inert impermeable solid particles can be accounted for. From the sensitivity analysis it became clear that for a given application, where the parameters  $m_R$ ,  $d_p$ ,  $\varepsilon$ ,  $\tau$ ,  $D_R$  are usually known, especially the position with respect to the interface remains as important factor. Since the enhancement factor increases almost exponentially with decreasing distance from the gas–liquid interface, it is not sufficient to assume the particles to be at some arbitrary distance from this interface (as e.g. in the models by Junker et al. [7,8], Holstvoogd et al. [10] and Vinke [24]). Statistical averaging over all positions, using the contribution to the enhancement as weighing factor is required, as in Eq. (8a,b) where the probability of finding a particle was taken the same for every position within the section of the film under consideration. When more than one particle needs to be taken into account, the sequential approach discussed in Section 5 is regarded as a good approximation.

The equal probability of finding a particle at a certain position may be influenced by settling effects, especially relevant for horizontal interfaces as e.g. encountered in a stirred cell [15] or by adhesion of particles to the interface [22,24]. This latter effect was found to be very important for slurry systems with activated carbon particles. Brownian motion of the small particles may counteract these settling effects



(a) Variation of  $d_p$  and hold-up  $\varepsilon$  ( $m_R = 10$ )



(b) Influence of  $d_p$  and  $m_R$  ( $\varepsilon = 0.10$ )

Fig. 12. Results for a homogeneous model. Conditions applied:  $m_R = 10$ ,  $\varepsilon = 0.10$ ,  $k_{GL} = 11.6 \cdot 10^{-5} \text{ (m s}^{-1}\text{)}$  and  $Sh = 2$  is used for the liquid–liquid mass transfer coefficient. (a) Variation of  $d_p$  and hold-up  $\varepsilon$  ( $m_R = 10$ ). (b) Influence of  $d_p$  and  $m_R$  ( $\varepsilon = 0.10$ ).

and will result in a more homogeneous distribution. This was studied experimentally for small (silica) particles near gas–liquid interfaces by Al-Naafa and Selim

[25] who found a value of  $3 \cdot 10^{-13} \text{ m}^2 \text{ s}^{-1}$  for the 'particle diffusion coefficient  $D'_o$ ' for  $1 \mu\text{m}$  particles, which is in good agreement with the Stokes–Einstein

Table 3  
Comparison of homogeneous and heterogeneous simulation results with experimental results

Experimental study	$m_R$	$D_R$	$\varepsilon$	$d_p$ ( $\mu\text{m}$ )	$k_L$ ( $\text{m s}^{-1}$ )	$E_{\text{exp}}$	$E_{\text{hom}}$	$E_{\text{het}}$
[15] (G–L–L, falling film exp.)	103	1.81	0.034	3.0	$11.6 \cdot 10^{-5}$	2.22	1.99	1.76
			0.187		$10.1 \cdot 10^{-5}$	4.14	4.34	4.16
[14] (Table 1 S–L–L, stirred cell)	8890	1.7 <sup>a</sup>	0.02	3.5	$9.8 \cdot 10^{-6}$	4.00	2.71	2.6
			0.05			6.73	5.69	4.4
			0.10			9.10	7.94	7.4
			0.20			12.00	11.07	12.7
[23] (S–L–S, agitated tank)	0	0	0.02	0.33	$4 \cdot 10^{-4}$	0.55	0.99	0.40
	{SiC}		0.02	$\approx 1$	$4 \cdot 10^{-4}$	0.68	0.99	0.89
	{Kaolin}					0.9		
	{Iron oxide}					0.63		
			0.02	$\approx 1$	$1 \cdot 10^{-4}$		0.99	0.66

<sup>a</sup> Estimated value.

relationship,  $D_o = k T / (3\pi\eta d_p)$ . With this, the average displacement of a particle due to Brownian motion during gas–liquid contact time  $\tau$  may be one to several microns. This would imply that in the small zone near the gas–liquid interface where the mass transfer enhancement is really determined ( $\approx 0-0.15 \cdot \delta_p < 10 \mu\text{m}$ ), the probability for each position is approximately equal.

From Figs. 12 and 13 and Table 3 it is clear that homogeneous and heterogeneous models yield significantly different simulation results, especially concerning the dependency of the enhancement factor on  $\varepsilon$  and  $d_p$ . It has been mentioned that the local geometry at the interface changes with increasing  $\varepsilon$ , causing a more or less linear dependency of  $E$  on  $\varepsilon$ . It should be remembered, however, that at increasing  $\varepsilon$ , the degree of saturation of the first particle does increase. At a certain moment, for finite, not too high capacity particles, a second or even third particle needs to be taken into account. This will, undoubtedly, lead to a leveling off of the  $E$ – $\varepsilon$  curve. Another pitfall is that at increasing hold-up of the dispersed phase the physical limit of a dense packed bed of particles at the interface will be reached. In that case, increasing  $\varepsilon$  can, physically, not lead to a reduction of the (average) distance of the first layer of particles towards the interface. Geometry of the particle and the packing will become important. For these situations 3-D models are indispensable.

Preliminary results obtained with a (2- and) 3-D model presently being developed are presented in Fig. 15 for a single spherical particle with the same physico-chemical properties as reported in Table 1, except for the particle diameter being  $3.0 \mu\text{m}$  and the (minimum) particle to interface distance,  $L$ , which was  $0.64 \mu\text{m}$  in these simulations. In this figure the enhancement factors at the gas–liquid interface on different radial positions from the projection of the center of the particle on the interface are presented for the 1-D model presented in the present study and for a 2- and 3-D model. A few very important aspects can be recognized from this figure. First of all,

the particle enhances mass transfer over an area largely exceeding its own projection on the gas–liquid interface. Further, and these effects are related, the enhancement factor at the center position increases in the sequence 1-D > 2-D > 3-D whereas, the degree of saturation of the particle (given percent-wise with respect to the maximum solubility in the legend) increases in the same sequence. The 2- and 3-D models, in fact Eqs. (4a), (4b)–(6) and (6b), were solved using an overlapping grid technique [26]. More results and details on the computational methods used will be presented by Brilman [27].

This preliminary figure illustrates that although the 1-D models give reasonable results, even though the physical situation is not represented completely in accordance with reality in the model, the development of 2- and, especially, 3-D models is required to investigate the near interface effects (and particle-particle interaction) more correctly.

New, very accurate experiments in dedicated equipment are however still required, not only to yield reliable data for verifying and comparing the models, but especially information on the specific interface phenomena are required for a more thorough understanding and for the development of the appropriate models. Therefore, in such experiments special attention should be paid to the hold-up of the dispersed phase and possible phase separation or adhesion effects at the interface and to the effect of the particle size distribution. From the analysis above it is clear that for particles located closely to the interface the 1-D, homogeneous and heterogeneous, models are oversimplified representations of a 3-D reality.

## 7. Conclusions

A 1-D, heterogeneous, instationary mass transfer model was developed to describe diffusion (with or without chemical reaction) in heterogeneous media. At



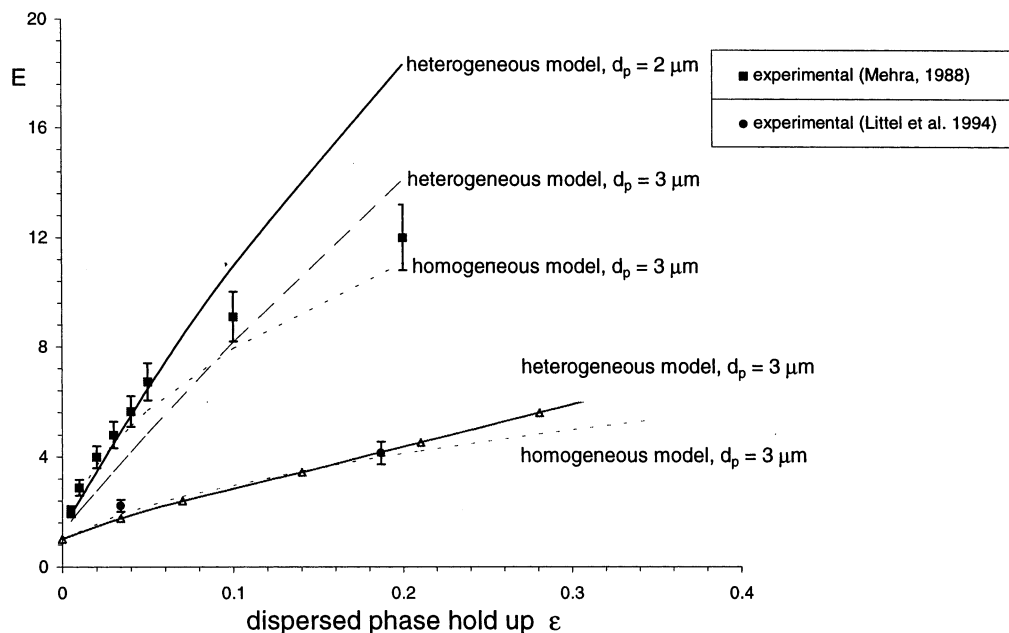


Fig. 13. Comparison of 1-D heterogeneous model with experimental results by Mehra [14] and Littel et al. [15].

conditions under which significant enhancement of mass transfer occurs, it was shown by multiparticle calculations that only those particles very close to the gas–liquid interface determine the mass transfer enhancement. Effects of among others the particle to interface distance and factors influencing the absorption capacity of the microparticles for the diffusing solute on the mass transfer enhancement were studied, showing the relative importance of the parameters.

A comparison of modeling results with experimental data yields a somewhat different behavior with respect

to the dependency of the absorption flux on the dispersed phase hold-up when compared to the homogeneous models due to the changing local geometry near the gas–liquid interface. In some cases heterogeneous models seem to describe the physical situation more correctly. Interpretation of the modeling results is somewhat more complicated since averaging over all possible configurations is required. Especially for multiparticle simulations these averaging techniques, or alternatively, the definition of a representative unit cell, need further consideration.

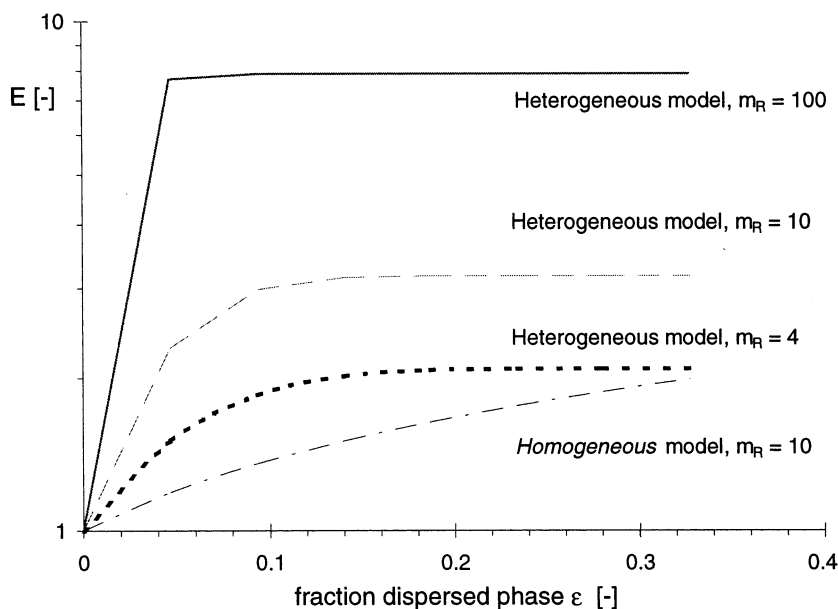


Fig. 14. Effect of leveling off of the enhancement factor at constant  $L_o$ .

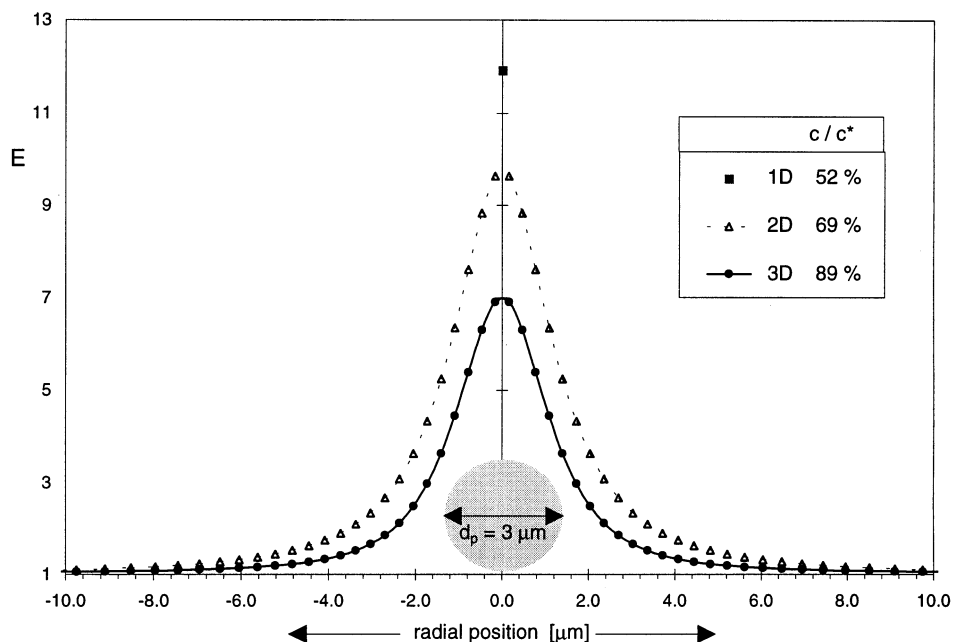


Fig. 15. Enhancement factors at different radial positions from the particle center for a 2- and 3-D model.

Considering that only those particles located very near the interface determine mass transfer, attention should be focused on these region. It is therefore believed that the developed 1-D heterogeneous model as well as the homogeneous models presented in literature remain first-approximation models due to their 1-D character. Two and especially 3-D mass transfer models should therefore be developed to investigate near interface effects and particle interaction. Experimental research investigating the near interface hold-up and the particle distribution within this zone is highly desirable, since it may yield essential information for understanding (and modeling) mass transfer phenomena in the presence of fine particles.

### Acknowledgements

The authors wish to thank M.J.V. Goldschmidt for his contribution to the modeling part and the SHELL Research and Technology Center in Amsterdam (The Netherlands) for the financial support.

### Appendix A. Nomenclature

$c$	concentration ( $\text{mol m}^{-3}$ )
$D$	diffusion coefficient ( $\text{m}^2 \text{s}^{-1}$ )
$D_R$	relative diffusion coefficient ( $D_d/D_c$ )
$d$	characteristic particle diameter (m)
$d_p$	particle diameter (m)

$E$	enhancement factor
$E_{c,c}$	enhancement factor due to chemical reaction in the continuous
$J$	mass transfer flux ( $\text{mol m}^{-2} \text{per s}$ )
$j^{av}$	average mass transfer flux for the heterogeneous cell (Eqs. (3a) and (3b)) ( $\text{mol m}^{-2} \text{per s}$ )
$k_1$	first order reaction rate constant ( $1/\text{s}$ )
$K_1$	liquid side mass transfer coefficient ( $\text{m s}^{-1}$ )
$L$	distance to the gas–liquid interface (m)
$L_o$	distance of first particle to the gas–liquid interface (multi-particle calc.) (m)
$m_R$	relative solubility or distribution coefficient ( $(\text{mol m}^{-3})_{LII}/(\text{mol m}^{-3})_{LI}$ )
$N$	number of particles in the mass transfer zone
$Ra$	reaction rate ( $\text{mol a m}^{-3} \text{per s}$ )
$R_D$	interparticle distance, Eqs. (1a) and (1b) (m)
$t$	time (s)
$x$	distance from gas–liquid interface (m)

#### Greek symbols

$\delta$	mass transfer zone near interface (m)
$\delta_p$	penetration depth (m)
$\varepsilon$	fraction dispersed phase
$\tau$	gas–liquid contact time (s)

#### Sub and superscripts

a	gas phase reactant a
b	liquid phase reactant b
av	average value
bulk	at bulk liquid phase conditions
c	continuous phase
d	dispersed phase

exp	experimental value
F	according to the film theory
het	heterogeneous (model)
hom	homogeneous (model)
p	physical absorption
ref	reference value
*	maximum solubility

## References

- [1] A.A.C.M. Beenackers, W.P.M. Van Swaaij, Mass transfer in gas–liquid slurry reactors, *Chem. Eng. Sci.* 48 (1993) 3109–3139.
- [2] R.L. Kars, R.J. Best, A.A.H. Drinkenburg, The sorption of propane in slurries of active carbon in water, *Chem. Eng. J.* 17 (1979) 201–210.
- [3] A. Mehra, A. Pandit, M.M. Sharma, Intensification of multiphase reactions through the use of a microphase-II. Experimental, *Chem. Eng. Sci.* 43 (1988) 913–927.
- [4] E. Alper, W.D. Deckwer, Comments on gas absorption with catalytic reaction, *Chem. Eng. Sci.* 36 (1981) 1097–1099.
- [5] J.T. Tinge, A.A.H. Drinkenburg, The enhancement of the physical absorption of gases in aqueous activated carbon slurries, *Chem. Eng. Sci.* 50 (1995) 937–942.
- [6] M. Nishikawa, T. Kayama, S. Nishioka, S. Nishikawa, Drop size distribution in mixing vessel with aeration, *Chem. Eng. Sci.* 49 (1994) 2379–2384.
- [7] B.H. Junker, D.I.C. Wang, A.H. Hatton, Oxygen transfer enhancement in aqueous/perfluorocarbon fermentation systems: I. Experimental observations, *Biotechnol. Bioeng.* 35 (1990) 578–585.
- [8] B.H. Junker, D.I.C. Wang, A.H. Hatton, Oxygen transfer enhancement in aqueous/perfluorocarbon fermentation systems: II. Theoretical analysis, *Biotechnol. Bioeng.* 35 (1990) 586–597.
- [9] E. Alper, B. Wichtendahl, W.D. Deckwer, Gas absorption mechanism in catalytic slurry reactors, *Chem. Eng. Sci.* 35 (1980) 217–222.
- [10] R.D. Holstvoogd, W.P.M. van Swaaij, L.L. van Dierendonck, The absorption of gases in aqueous activated carbon slurries enhanced by adsorbing or catalytic particles, *Chem. Eng. Sci.* 43 (1988) 2182–2187.
- [11] R.D. Holstvoogd, W.P.M. van Swaaij, The influence of adsorption capacity on enhanced gas absorption in activated carbon slurries, *Chem. Eng. Sci.* 45 (1990) 151–162.
- [12] A. Mehra, Gas absorption in slurries of finite capacity microphases, *Chem. Eng. Sci.* 46 (1990) 1525–1538.
- [13] W.J. Bruining, G.E.H. Joosten, A.A.C.M. Beenackers, H. Hofman, Enhancement of gas–liquid mass transfer by a dispersed second liquid phase, *Chem. Eng. Sci.* 41 (1986) 1873–1877.
- [14] A. Mehra, Intensification of multiphase reactions through the use of a microphase-I. Theoretical, *Chem. Eng. Sci.* 43 (1988) 899–912.
- [15] R.J. Littel, G.F. Versteeg, W.P.M. Van Swaaij, Physical absorption of CO<sub>2</sub> and propene into toluene/water emulsions, *A.I.Ch.E. J.* 40 (1994) 1629–1638.
- [16] E. Nagy, A. Moser, Three-phase mass transfer: Improved pseudo-homogeneous model, *A.I.Ch.E. J.* 41 (1995) 23–34.
- [17] C.J. van Ede, R. Van Houten, A.A.C.M. Beenackers, Enhancement of gas to water mass transfer rates by a dispersed organic phase, *Chem. Eng. Sci.* 50 (1995) 2911–2922.
- [18] S. Karve, V.A. Juvekar, Gas absorption into slurries containing fine catalyst particles, *Chem. Eng. Sci.* 45 (1990) 587–594.
- [19] E. Nagy, Three-phase mass transfer: One dimensional heterogeneous model, *Chem. Eng. Sci.* 50 (1995) 827–836.
- [20] J. Crank, *Mathematics of Diffusion*, Oxford University Press, Oxford, 1976.
- [21] K.R. Westerterp, W.P.M. Van Swaaij, A.A.C.M. Beenackers, *Chemical Reactor Design and Operation*, Wiley, 1993.
- [22] O.J. Wimmers, J.M.H. Fortuin, The use of adhesion of catalyst particles to gas bubbles to achieve enhancement of gas absorption in slurry reactors, *Chem. Eng. Sci.* 43 (1988) 303–312.
- [23] K.S. Geetha, G.D. Surender, Solid–liquid mass transfer in the presence of microparticles during dissolution of iron in a mechanically agitated reactor, *Hydrometallurgy* 36 (1994) 231–246.
- [24] H. Vinke, The effect of catalyst particle to bubble adhesion on the mass transfer in agitated slurry reactors, Ph.D. thesis, Municipal University of Amsterdam, 1992 (The Netherlands).
- [25] M.A. Al-Naafa, M. Sami Selim, Sedimentations and Brownian diffusion coefficients of interacting hard spheres, *Fluid Phase Equilibria* 88 (1993) 227–238.
- [26] G. Chesshire, W.D. Henshaw, Composite overlapping meshes for the solution of partial differential equations, *J. Comp. Ph.* 90 1–64.
- [27] D.W.F. Brilman, Thesis University of Twente, The Netherlands, 1998 (to be published).